22ND INTERNATIONAL WORKSHOP
ON LASER RANGING

7-11 November 2022
Yebes, Spain

RECONNECTING THE ILRS COMMUNITY

WROCŁAW UNIVERSITY
OF ENVIRONMENTAL
AND LIFE SCIENCES

Tropospheric delay modeling in SLR solutions based on numerical weather models and the estimation of tropospheric bias corrections

Mateusz Drożdżewski, Krzysztof Sośnica,
Dariusz Strugarek, Radosław Zajdel, Grzegorz Bury

Systematic errors in SLR (geometry)

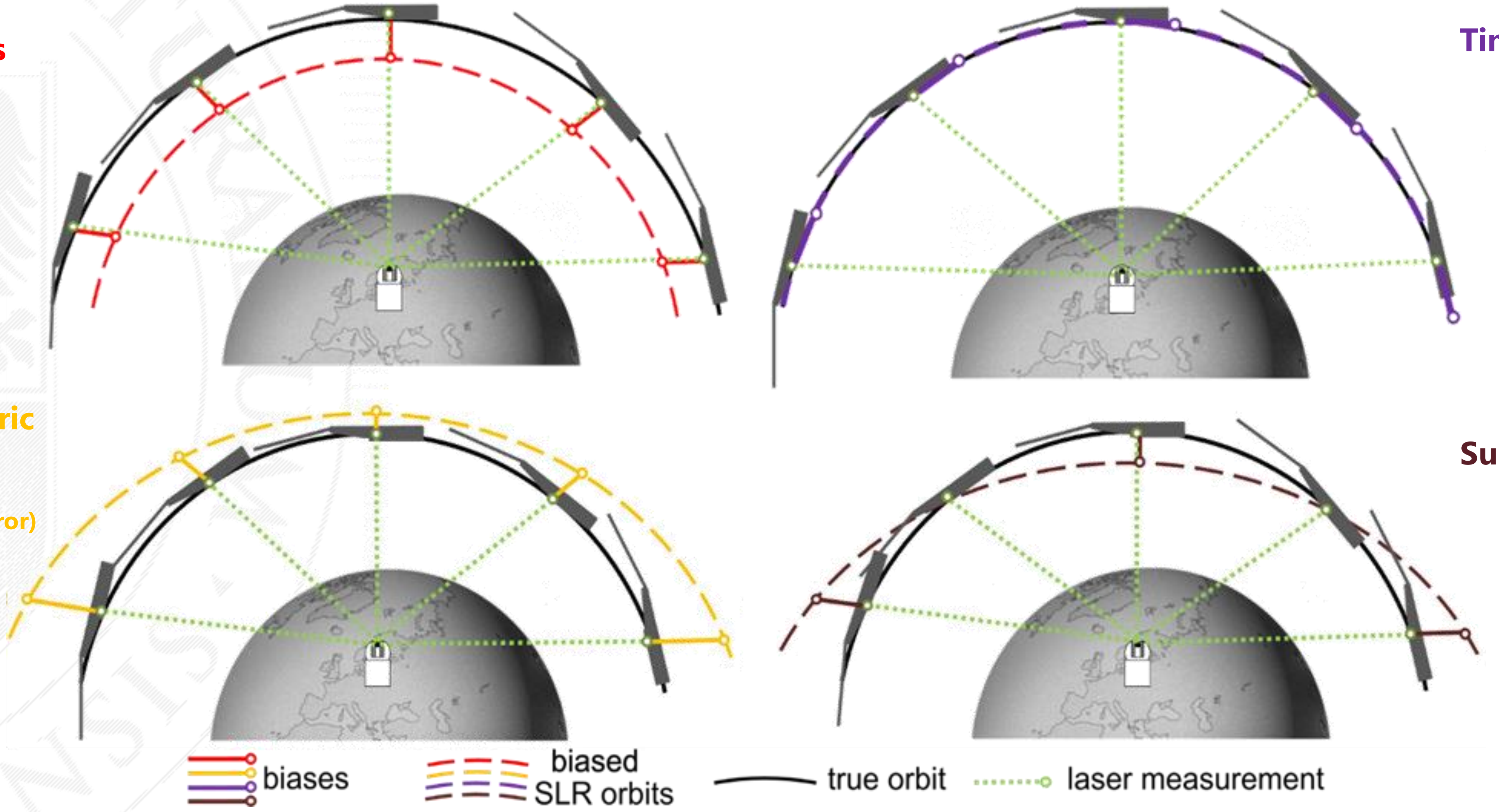

Range bias

Time bias

Tropospheric bias
(elevation-dependent error)

Sum of errors

SLR validation of SWARM GPS-based orbits (Graz station, Austria)

Original data

Reprocessed data (with a bias correction)

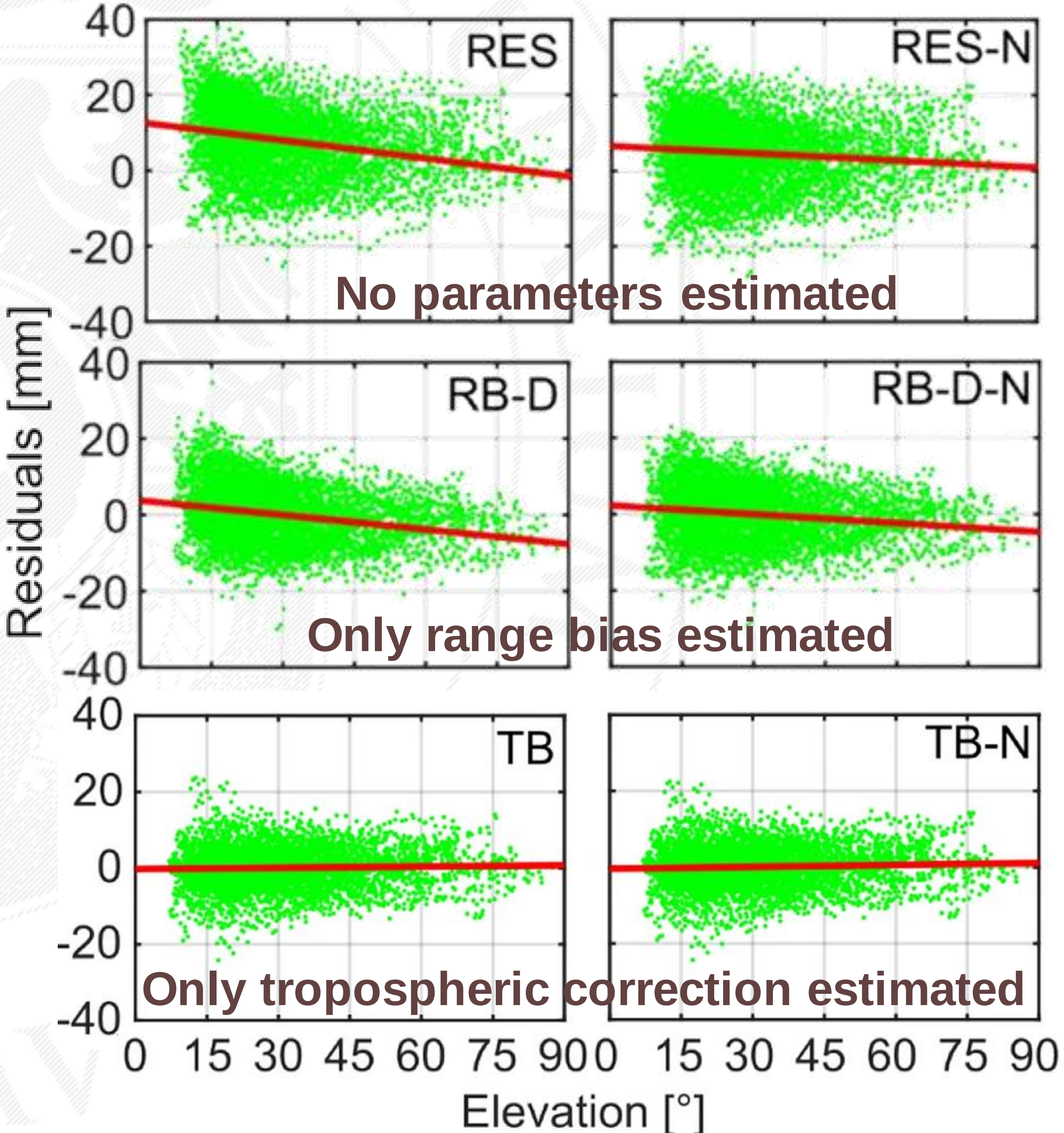

Wang et al. (2020) reported an offset and drift in barometer measurements installed at the Graz station, which affected the troposphere correction.

The barometer data for Graz have been reprocessed and observations with new barometer data are now available at the ILRS Data Centers.

1. The estimation of range biases reduces the mean offset of SLR residulas to zero. However, range biases do not remove the elevation dependency of the observation residulas.
2. The estimation of tropospheric corrections (one parameter per station) removes the zenith offset and elevation-dependent biases.

Strugarek et al. (2022) ***Satellite Laser Ranging to GNSS-based Swarm orbits with handling of systematic errors***, GPS Solutions, 26(104) https://doi.org/10.1007/s10291-022-01289-1

Observation geometry & correlations

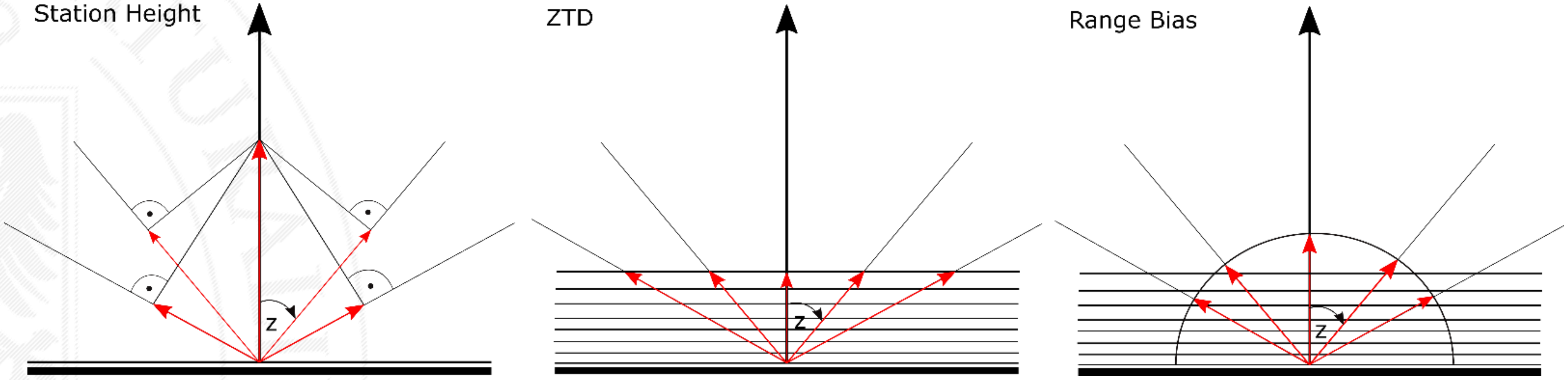

$$\delta\rho_h = -\cos(z) * \delta\rho_h(0)$$

$$\delta\rho_{trp}(z) = mfs(z) * \delta\rho_{trp}(0)$$

$$\delta\rho_{RB}(z) = \delta\rho_{RB}(0)$$

In SLR, zenith tropospheric delay (ZTD), station heights, and range biases are correlated.

The correlation is strongest when only few observations are collected at low elevation angles, e.g., for high-orbiting satellites.

Station heights are one of the most important parameters, because the scale of the reference frame, geocenter motion, and many other parameters rely on the station heights.

A wrong tropospheric delay affects the estimation of station heights because of the correlations.

Artificial pressure bias – a simulation

- We apply a 5 hPa pressure bias to all SLR stations
- 5 hPa translates into ~11.4 mm differences in tropospheric zenith delay
- We use station coordinates from a standard solution (without a pressure bias) as a priori values
- We examine following scenarios using real LAGEOS-1/2 observations for 2010-2019:

Estimated parameters / solution	Range bias (RB)	Troposphere zenith delay (TRP)	Station coordinates (CRD)
NEU			x
RB+NEU	x		x
TRP+NEU		x	x
TRP+RGB+NEU	x	x	x

Drożdżewski M., Sośnica K. (2021) ***Tropospheric and range biases in Satellite Laser Ranging***
Journal of Geodesy, Vol. 95 No. 100, DOI: 10.1007/s00190-021-01554-0

Artificial pressure bias – a simulation

Graz - 7839

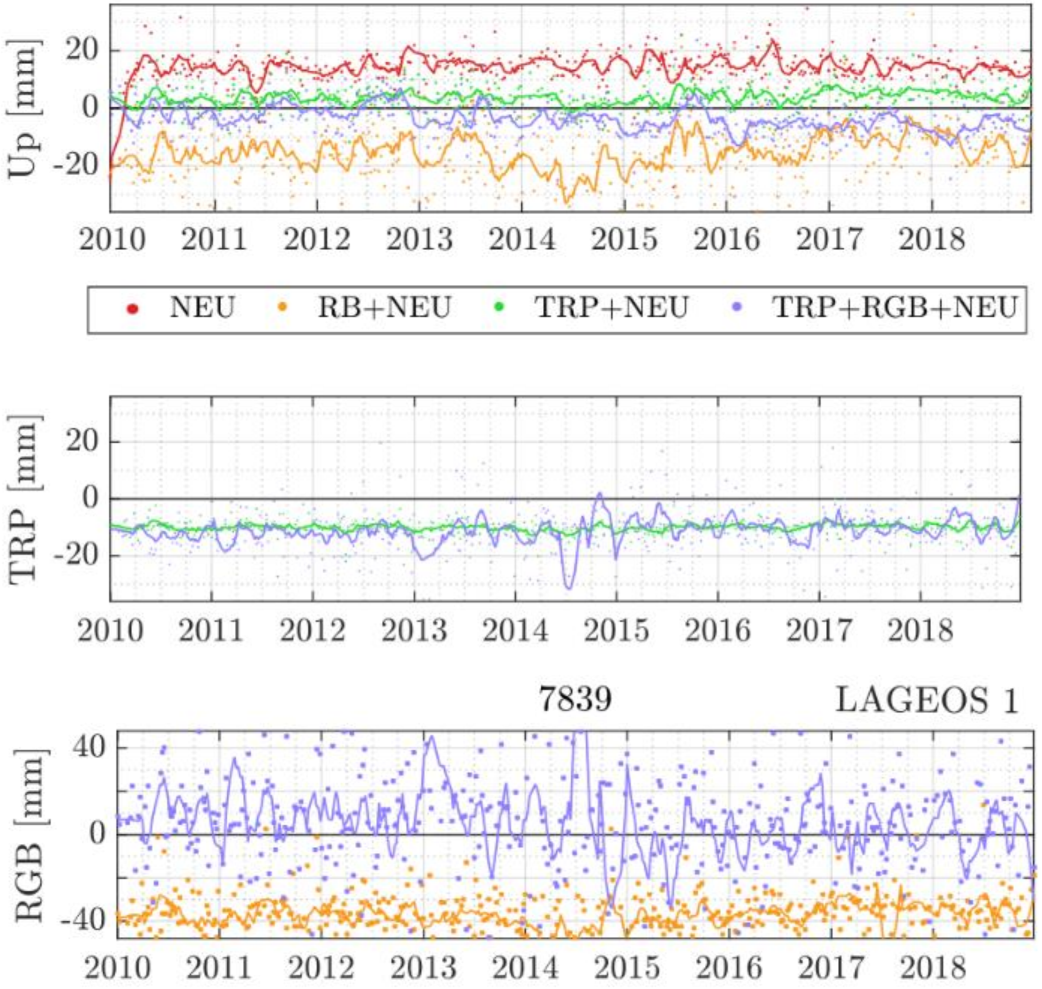

5 hPa (11.4 mm of ZTD) causes a systematic error at the level of +15 mm in station heights (red)

When estimating range biases and coordinates (RB+NEU, orange), the mean bias is **-16 mm.**

Estimation of troposphere delay corrections properly reconstructs ~90% of the pressure bias (there is a remaining error of 1-2 mm).

Solutions with estimated troposphere delay correction are more consistent with a priori coordinates derived from standard solution.

When trying to capture the tropospheric bias by estimating a range bias, the resulting RB value is -40 mm (orange), but the station height is wrong by -16 mm.

Drożdżewski M., Sośnica K. (2021) ***Tropospheric and range biases in Satellite Laser Ranging.*** Journal of Geodesy, Vol. 95 No. 100, DOI: 10.1007/s00190-021-01554-0

Station heights affected by a 5 hPa bias

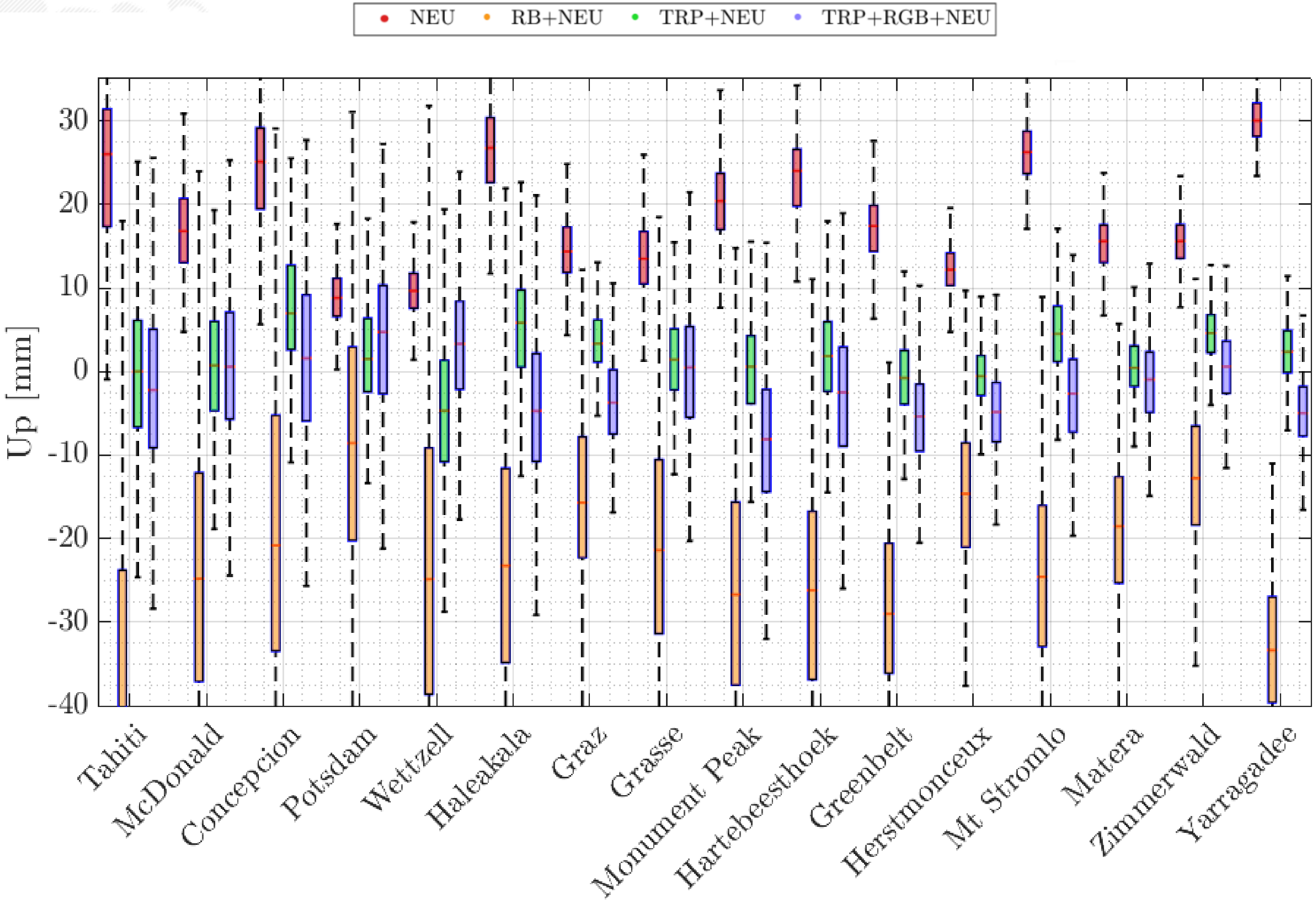

NEU ≈ 17 mm

TRP + NEU ≈ 1.5 mm

TRP + RGB + NEU ≈ -2.4 mm

RGB + NEU ≈ -24 mm

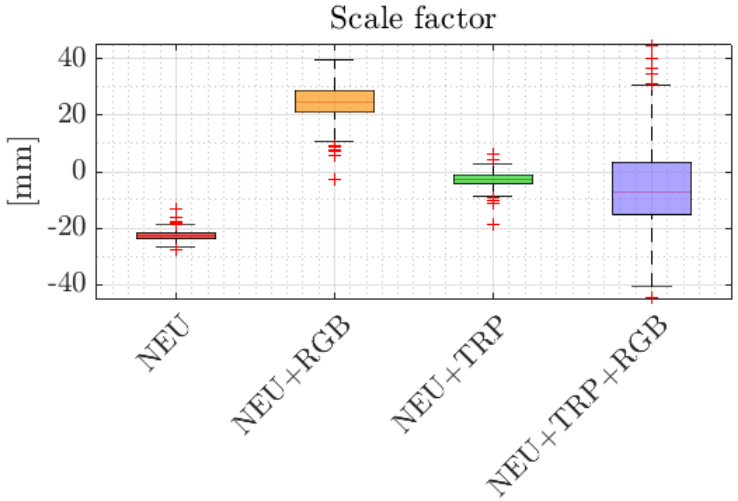

The Up station component with respect to the unbiased solution, for the period 2010 – 2019.

Time series of: TRP, RGB and Up component – without an artificial bias

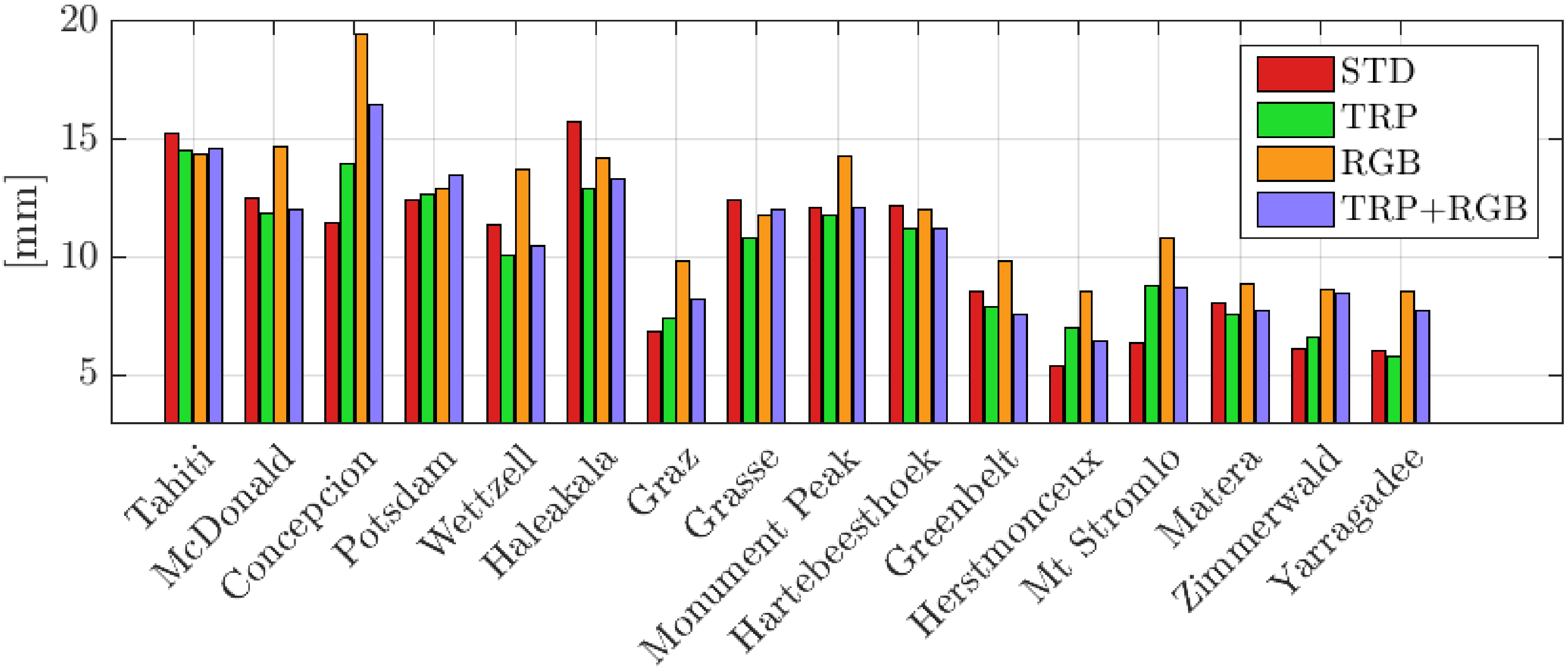

Interquartile ranges of the estimated up component of station coordinates

- Solution RGB significantly deteriorates the solution for more than 80 % of analyzed stations,
- Solution TRP improves 50 % of analyzed stations, whereas for 19 % we observe no significant difference.

Geocenter coordinates

- RGB and TRP significantly change the mean geocenter offset by more than 1 mm for the Y and Z components,

- The amplitude of the annual signal in the geocenter motion are only marginally changed,

- Uncalibrated biases substantially affect the geocenter coordinates, which are one of the fundamental products from SLR.

	X [mm]		Y [mm]		Z[mm]	
Solution	offset	amplitude	offset	amplitude	offset	amplitude
STD	0.3	2.6	1.9	2.1	-0.2	4.1
TRP	0.4	2.7	1.3	2.2	-1.6	3.8
RGB	0.3	3.0	0.7	2.3	-1.5	3.8
TRP+RGB	0.6	2.8	1.0	2.3	-1.4	3.7

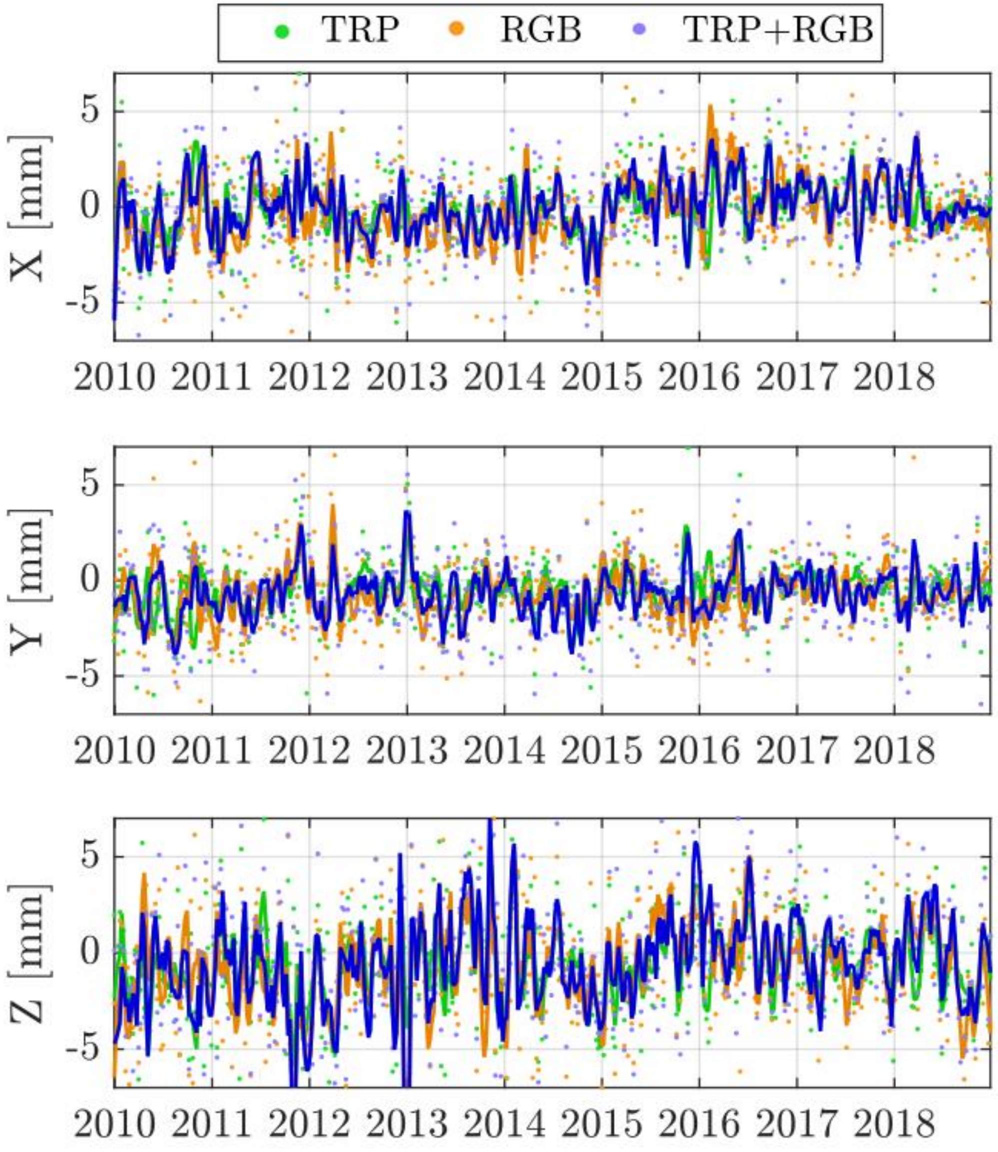

Differences of time series of geocenter coordinates w.r.t. the STD solution. The solid line corresponds to values based on the Savitzky-Golay filter with 3-month windowing.

Comparison of the first-order horizontal gradients of the troposphere delay

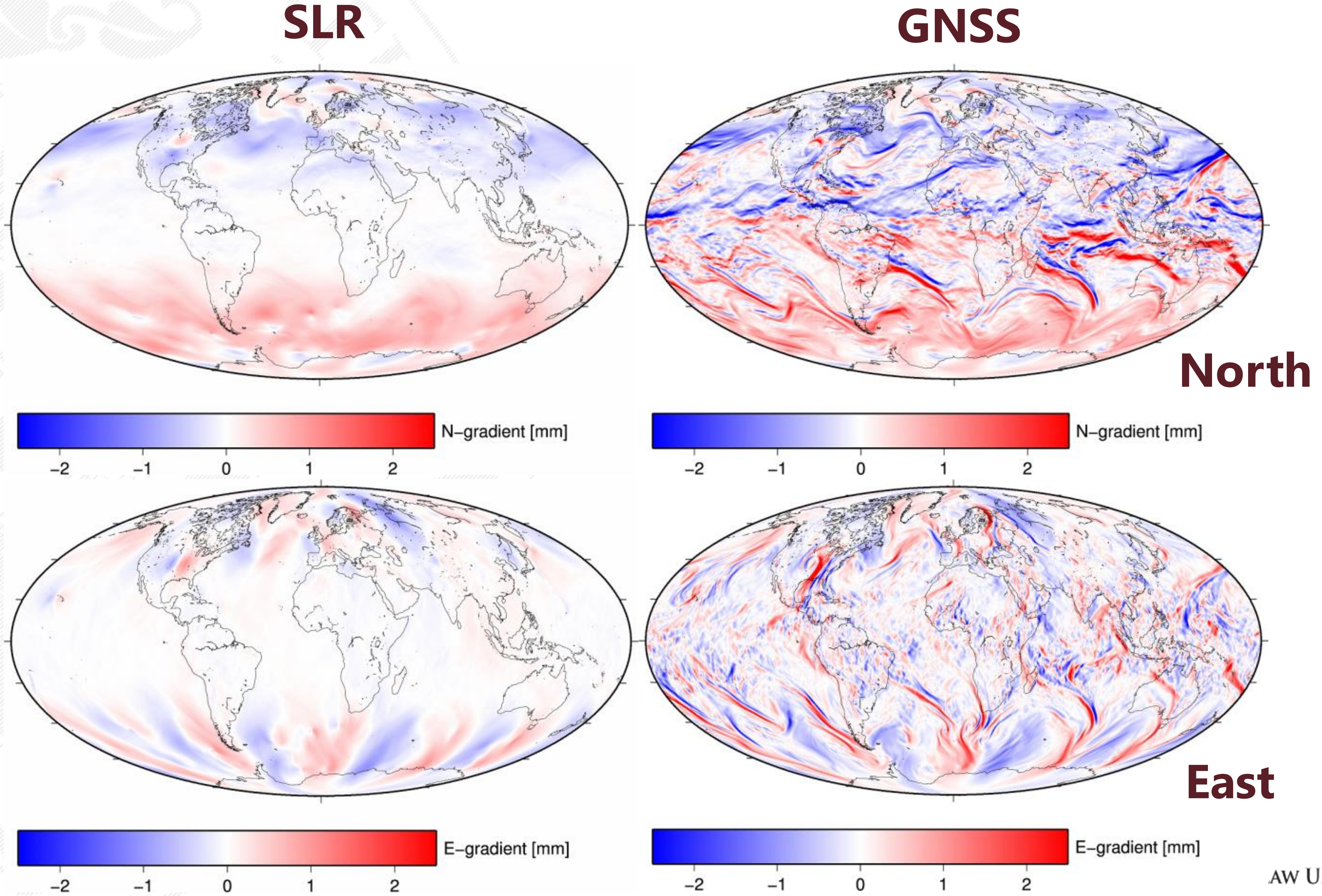

Gradients for SLR show thus smaller viariability in time when compared to GNSS gradients, because they are less sensitive to the water varpur content in the atmosphere. The long-term mean gradients assume similar values in SLR and GNSS solutions for the hydrostatic part. The GNSS-derived gradients cannot be directly applied for SLR.

Drożdżewski M., Sośnica K., Zus F., Balidakis K. (2019) *Troposphere delay modeling with horizontal gradients for Satellite Laser Ranging*. Journal of Geodesy. DOI https://doi.org/10.1007/s00190-019-01287-1

Numerical weather models (NWM)

WROCŁAW UNIVERSITY OF ENVIRONMENTAL AND LIFE SCIENCES

PMF (Potsdam Mapping Function) for SLR

GFZ
Helmholtz Centre
POTSDAM

- based on ERA5 (the latest version)
- a common mapping function and zenith delay for hydrostatic and wet delay
- includes first order and higher-order gradient terms
- provides tabular values for mapping function: *a, b, c*

VMF3o (Vienna Mapping Function for optical frequencies)

TU WIEN
TECHNISCHE UNIVERSITÄT WIEN
Vienna | Austria

- based on operational ERA and reprocessed ERA5 products
- separates hydrostatic and wet delays for the zenith delays and mapping fuctions
- includes first order gradient terms with a separation bewteen wet and dry parts
- provides tabular values for mapping function: *a* (wet and dry), whereas *b* and *c* are provided as an expansion into spherical harmonics
- provides tropospheric data (temperature, pressure, water varpour)

Simple model of gradients?

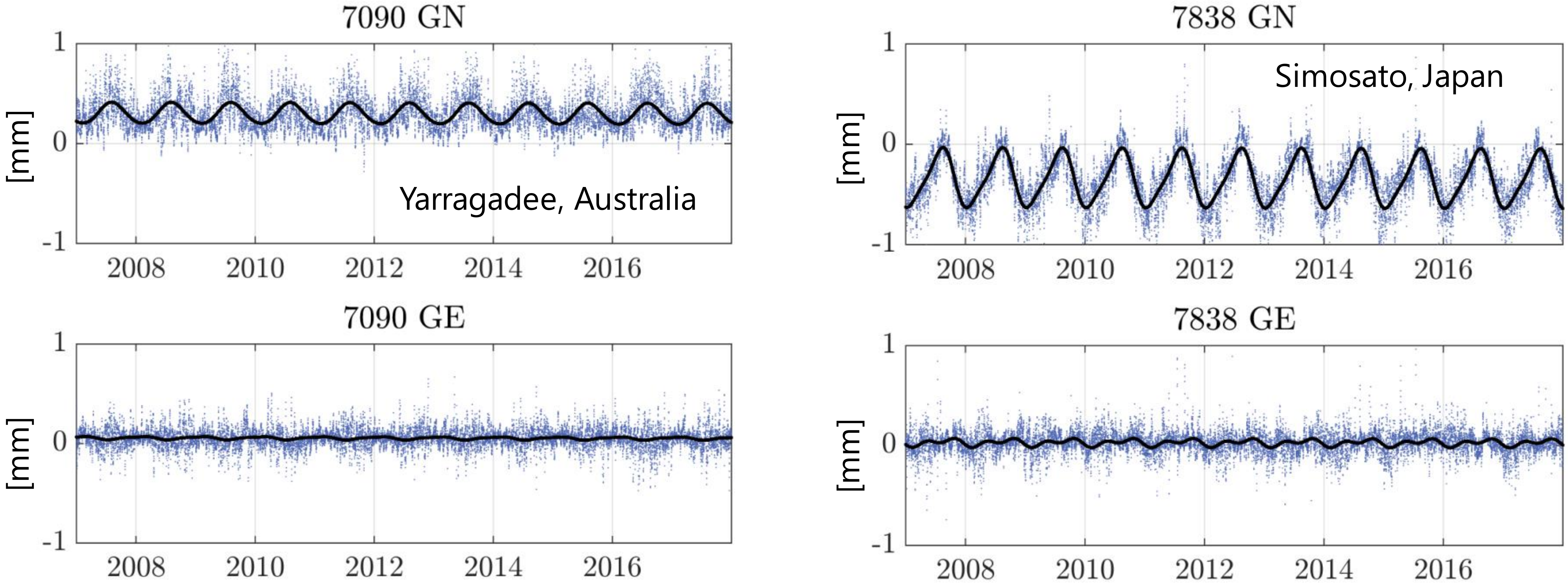

$$f(t) = a_0 + a_1 t + a_{s1}\sin\left(\frac{2\pi}{T}t\right) + a_{c1}cos\left(\frac{2\pi}{T}t\right) + a_{s2}\sin\left(\frac{4\pi}{T}t\right) + a_{c2}cos\left(\frac{4\pi}{T}t\right)$$

Offset + drift + annual signal + semi-annual signal for each component for each SLR station

Simple model of gradients?

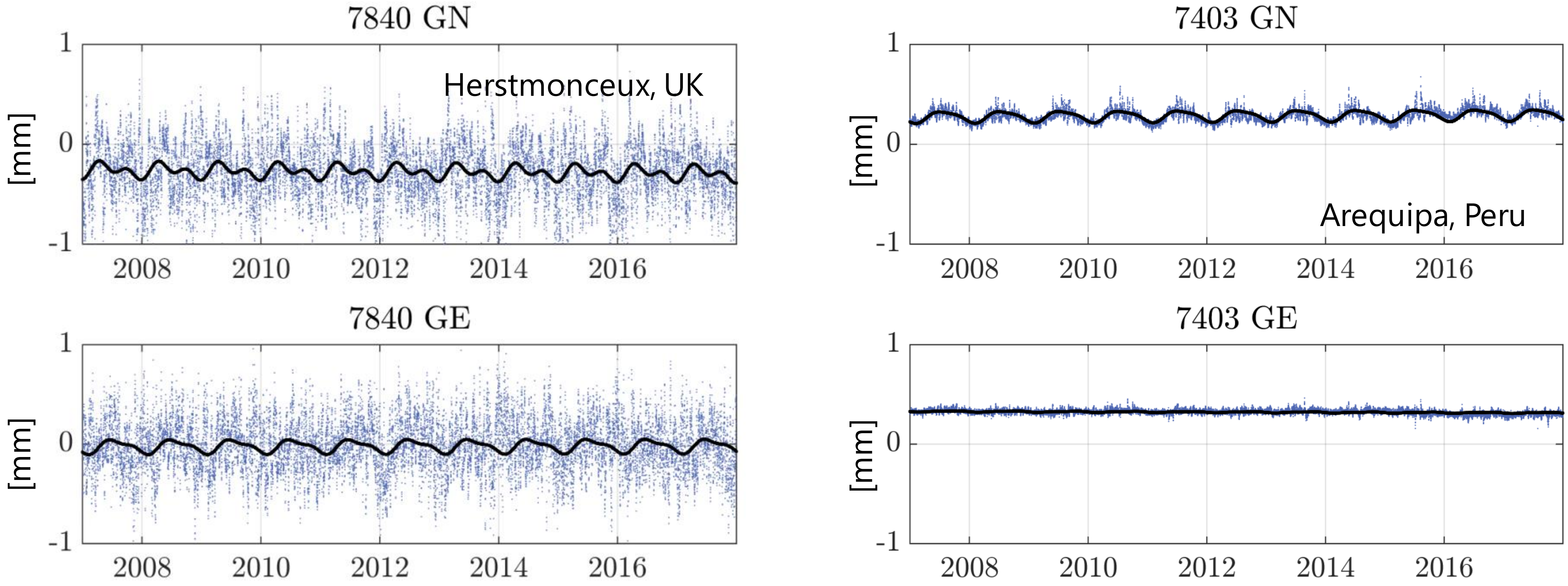
7840 GN

Herstmonceux, UK

7403 GN

Arequipa, Peru

7840 GE

7403 GE

$$f(t) = a_0 + a_1 t + a_{s1} \sin\left(\frac{2\pi}{T} t\right) + a_{c1} cos\left(\frac{2\pi}{T} t\right) + a_{s2} \sin\left(\frac{4\pi}{T} t\right) + a_{c2} cos\left(\frac{4\pi}{T} t\right)$$

Offset + drift + annual signal + semi-annual signal for each component for each SLR station

Differences Earth Rotation Parametrs due to including horizontal gradients

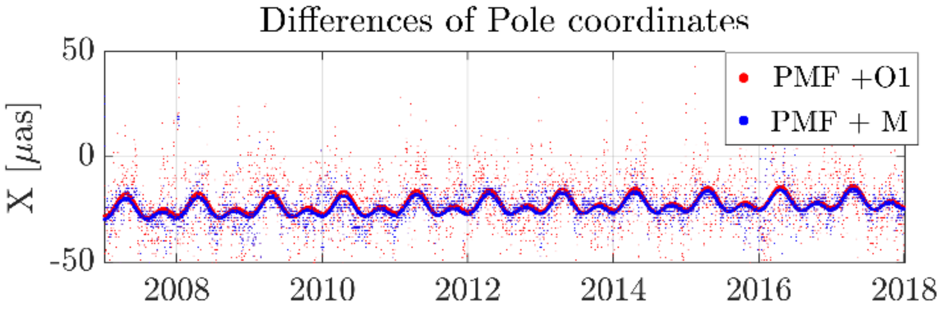

Difference in X-Pole = 20 µas

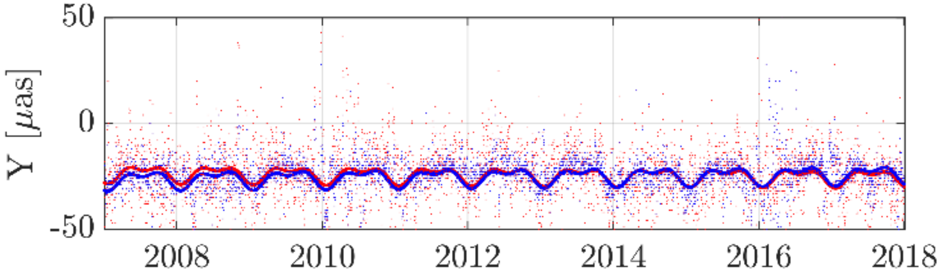

Difference in Y-Pole = 24 µas

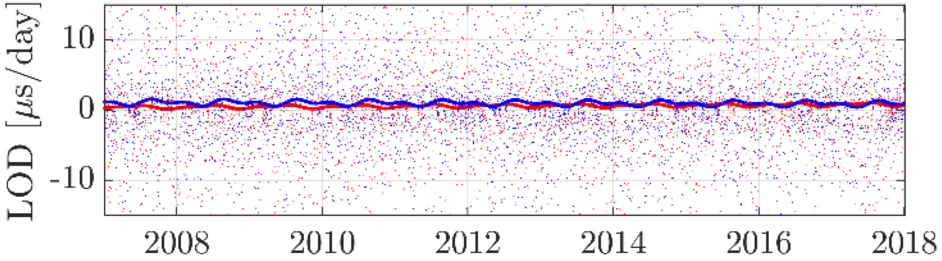

Figures show differences w.r.t. standard SLR solution, i.e., Mendes-Pavlis with no gradients.
Table shows differences w.r.t. IERS-14-C04 series.

Mean long-term offsets of X and Y pole coordinates are reduced by 20 µas. SLR solutions become more consistent with IERS-14-C04 combined series, which means that SLR solutions become more consistent with other techniques of space geodesy.

SLR w.r.t. IERS-14-C04	X-POLE		Y-POLE		LOD		No of ERP Sol.
	offset	σ	offset	σ	offset	σ	
	(µas)		(µas)		(µs/day)		
Mendes-Pavlis	**22**	7	**38**	8	-77	5	574
PMF	**23**	7	**38**	8	-77	5	574
PMF + GRAD	**2**	7	**14**	8	-76	5	574
PMF +M GRAD	**7**	8	**11**	8	-75	5	574

VMF3o pressure records as an independent ”barometer”

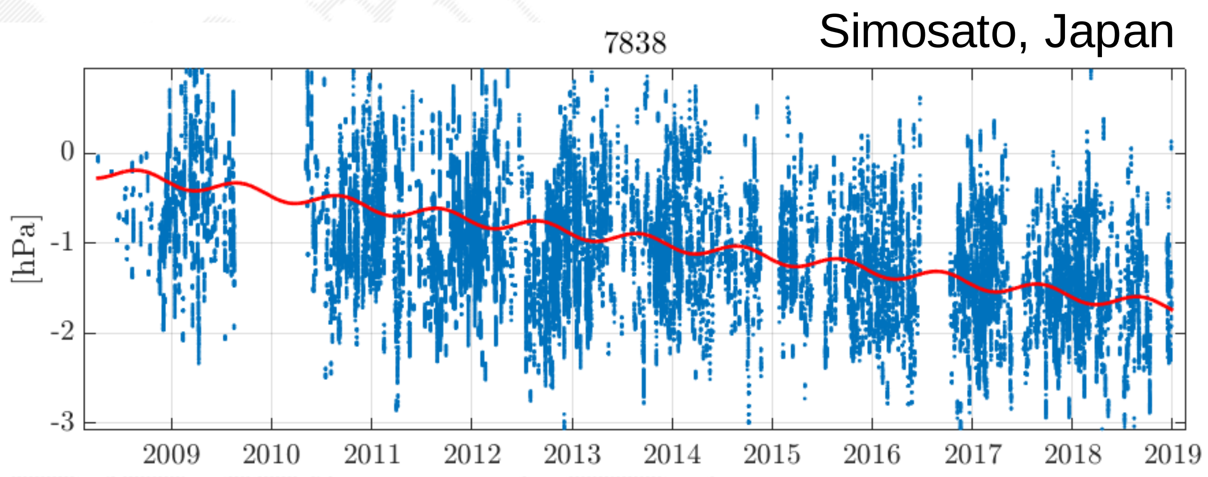
Simosato, Japan

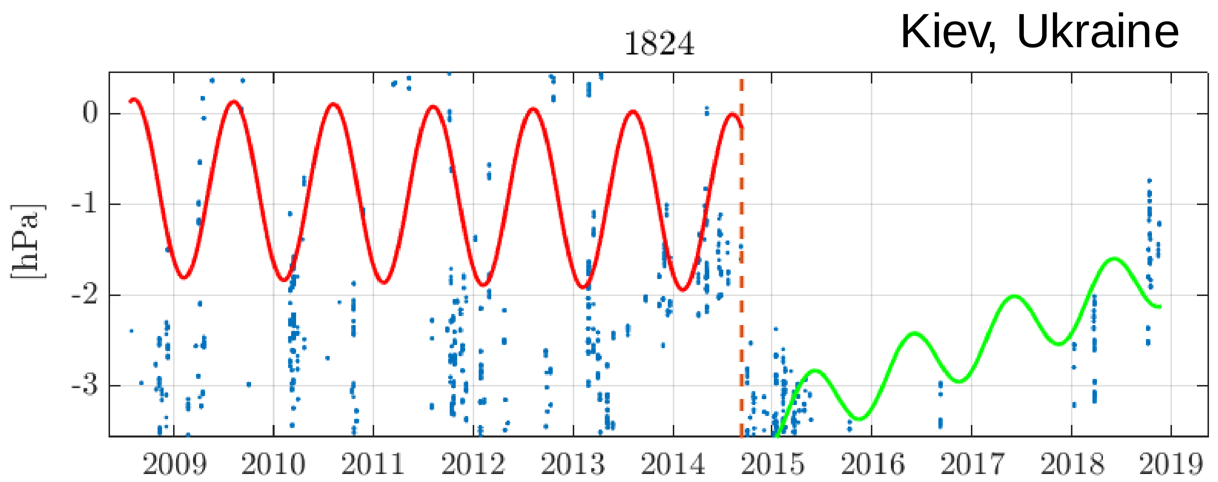
Kiev, Ukraine

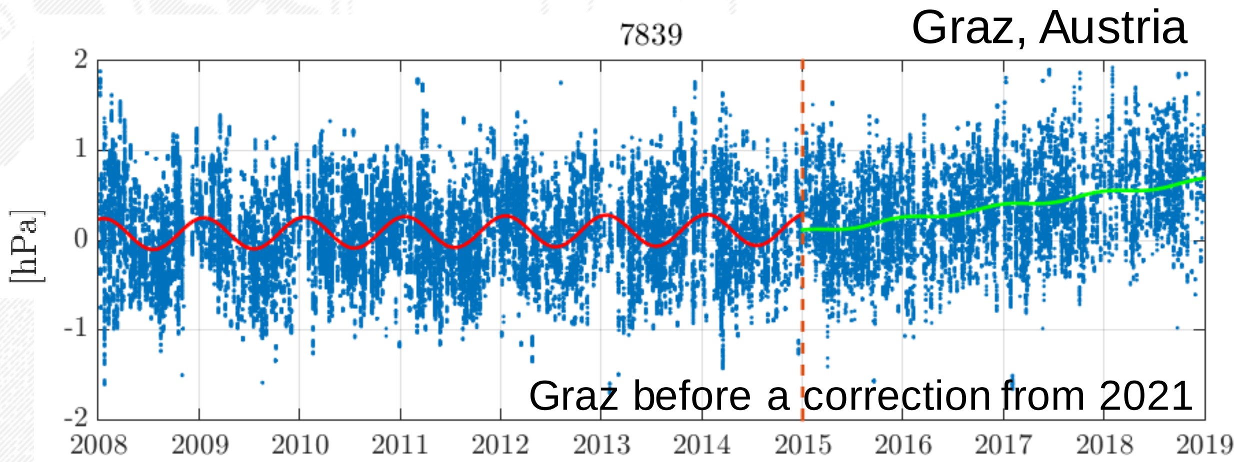
Graz, Austria

Graz before a correction from 2021

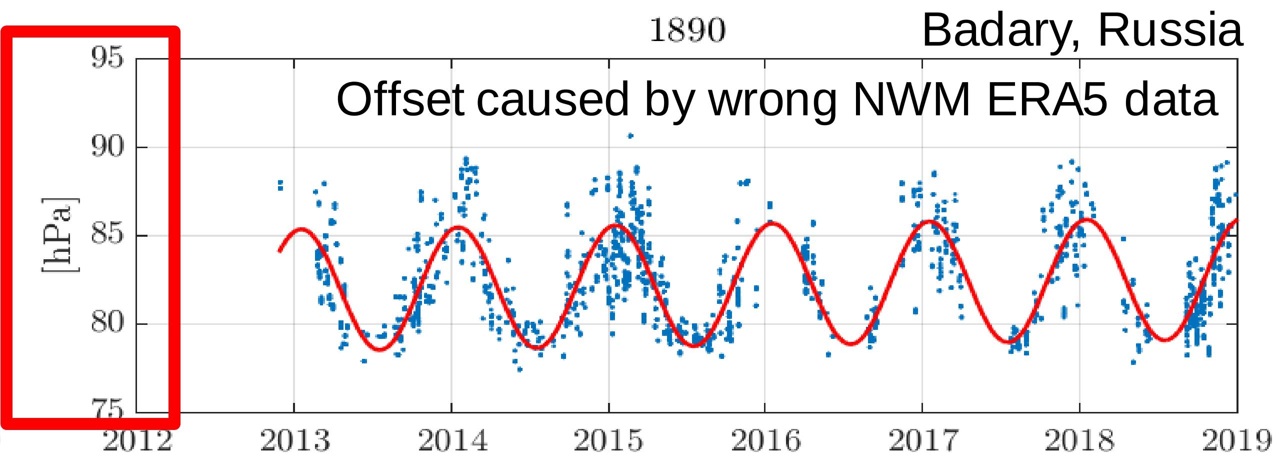
Badary, Russia

Offset caused by wrong NWM ERA5 data

Difference of pressure records derived from in-situ measurements and VMF3o: J. Boisits, D. Landskron and J. Boehm, ***VMF3o: the Vienna Mapping Functions for optical frequencies***. J Geod (2020). https://doi.org/10.1007/s00190-020-01385-5

VMF3o pressure records as an independent ”barometer”

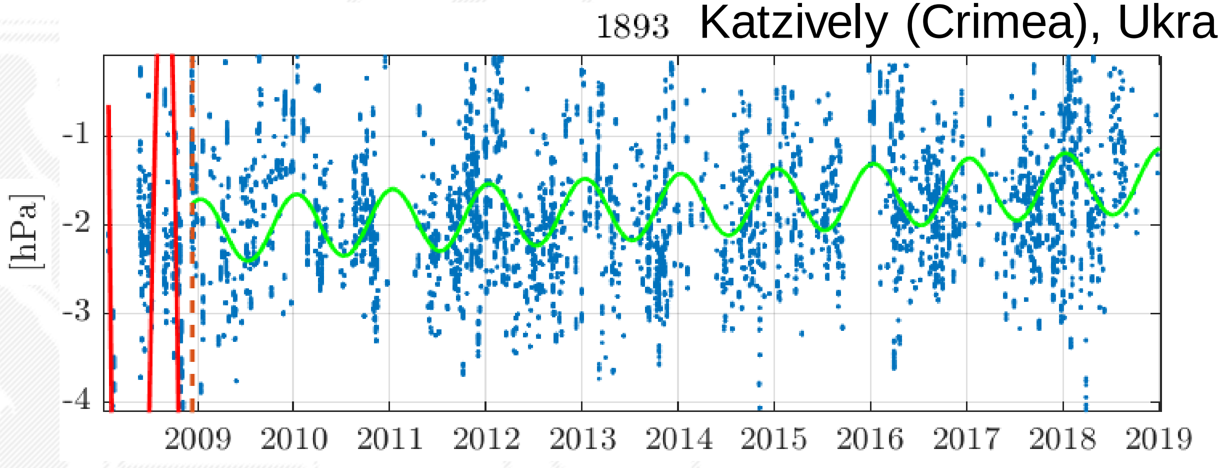

Katzively (Crimea), Ukraine

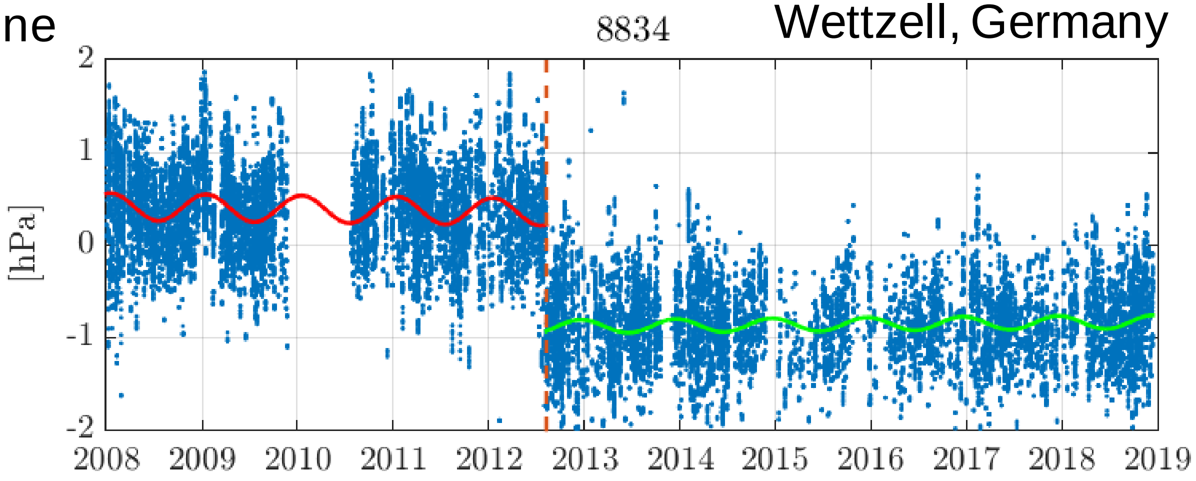

Wettzell, Germany

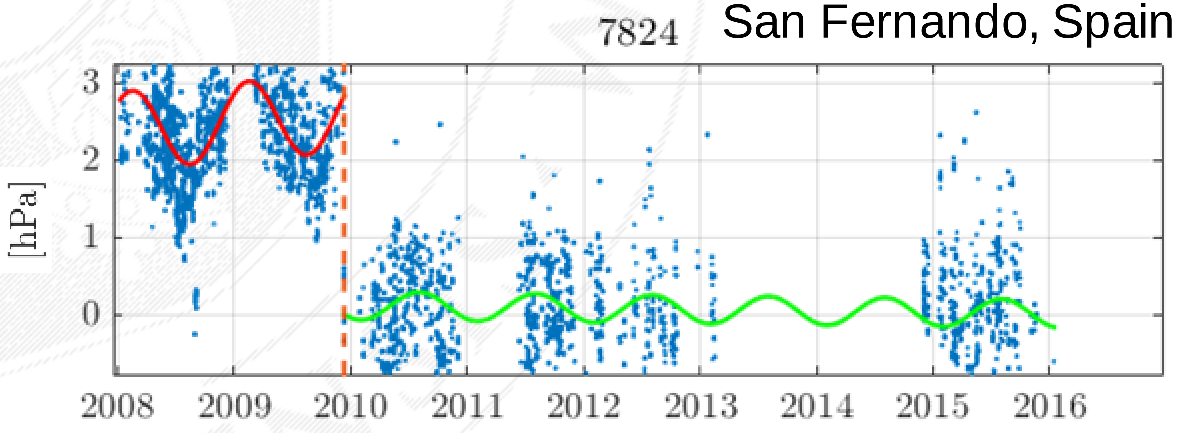

San Fernando, Spain

We cannot claim that the NWM are better than in-situ barometer data, however, the differences between in-situ and NWM data (offsets, trends, jumps) can indicate problems with barometers (or the numerical model).

Cross-check is much expected.

Conclusions

- Some SLR stations are affected by **barometer biases**, which can be mitigated by estimating tropospheric delay corrections.
- **Barometer biases** cannot be mitigated by estimating **range biases** due to their elevation-dependent nature. Range biases make the situation **even worse** (wrong up station coordinates).
- **Barometer biases** affect the **geocenter coordinates** and the **scale**.

- The **horizontal gradients** in SLR solutions should be based on numerical weather models (e.g., VMF3o, PMF, or a simple parametric model); the estimation of gradients should be avoided due to low number of data. The gradients should be considered at least for LAGEOS and lower satellites.
- **Gradients** affect the estimated **Earth rotation parameters** (e.g., pole coordinates).
- **In-situ meteorological** data are good for **zenith delays** (point data); however, **mapping functions and gradients** require meteo information on the surroundings of the station, which is better in **NWM**.

Thank you for your attention!

Special thanks to K. Balidakis, F. Zus,

J. Böhm, and J. Boisits for providing PMF and VMF

Krzysztof Sośnica

krzysztof.sosnica@upwr.edu.pl

Source code (in FORTRAN) and the station-specific tables are prepared

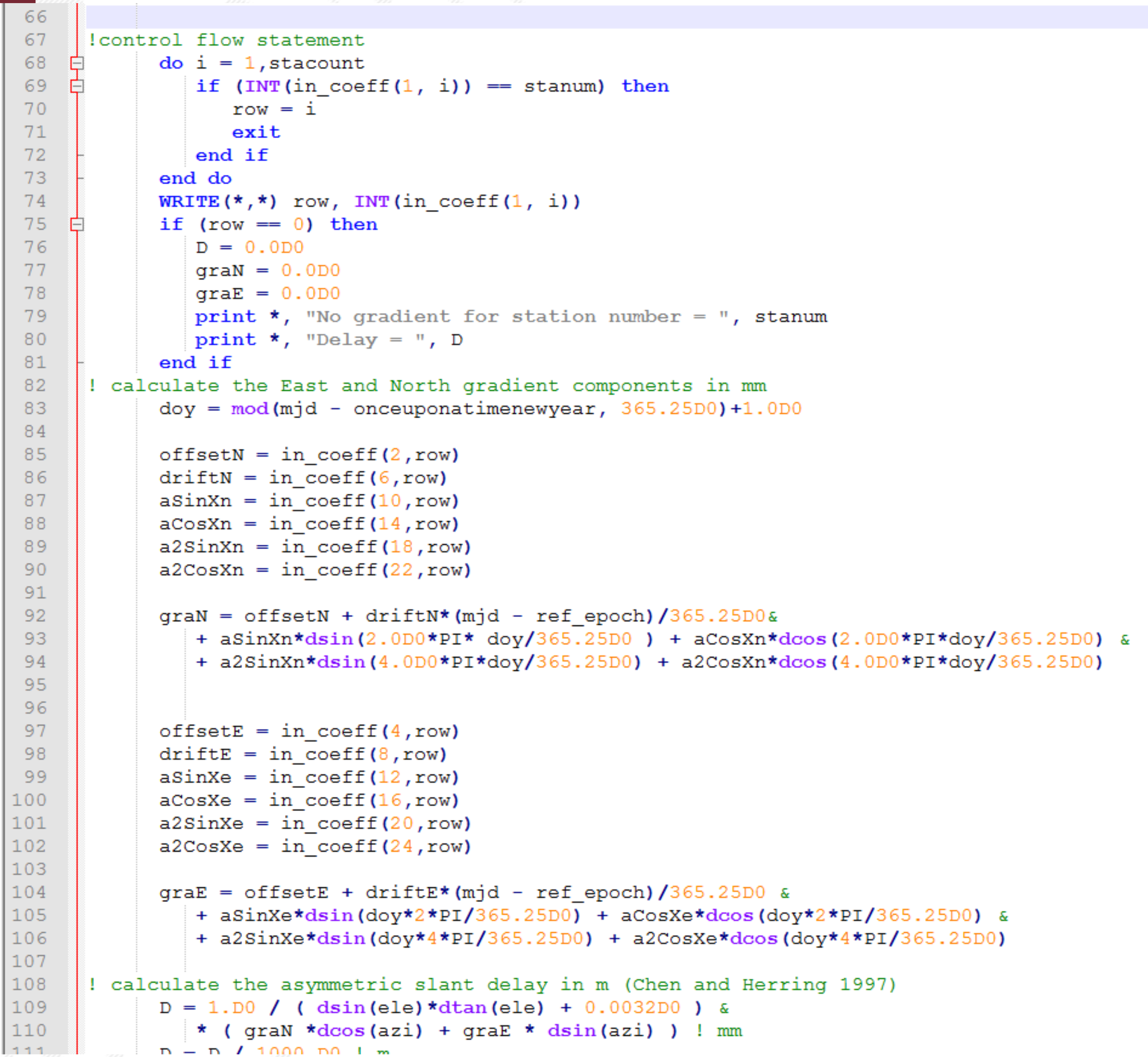

```fortran

!control flow statement
      do i = 1,stacount
         if (INT(in_coeff(1, i)) == stanum) then
            row = i
            exit
         end if
      end do
      WRITE(*,*) row, INT(in_coeff(1, i))
      if (row == 0) then
         D = 0.0D0
         graN = 0.0D0
         graE = 0.0D0
         print *, "No gradient for station number = ", stanum
         print *, "Delay = ", D
      end if
! calculate the East and North gradient components in mm
      doy = mod(mjd - onceuponatimenewyear, 365.25D0)+1.0D0

      offsetN = in_coeff(2,row)
      driftN = in_coeff(6,row)
      aSinXn = in_coeff(10,row)
      aCosXn = in_coeff(14,row)
      a2SinXn = in_coeff(18,row)
      a2CosXn = in_coeff(22,row)

      graN = offsetN + driftN*(mjd - ref_epoch)/365.25D0&
         + aSinXn*dsin(2.0D0*PI* doy/365.25D0 ) + aCosXn*dcos(2.0D0*PI*doy/365.25D0) &
         + a2SinXn*dsin(4.0D0*PI*doy/365.25D0) + a2CosXn*dcos(4.0D0*PI*doy/365.25D0)


      offsetE = in_coeff(4,row)
      driftE = in_coeff(8,row)
      aSinXe = in_coeff(12,row)
      aCosXe = in_coeff(16,row)
      a2SinXe = in_coeff(20,row)
      a2CosXe = in_coeff(24,row)

      graE = offsetE + driftE*(mjd - ref_epoch)/365.25D0 &
         + aSinXe*dsin(doy*2*PI/365.25D0) + aCosXe*dcos(doy*2*PI/365.25D0) &
         + a2SinXe*dsin(doy*4*PI/365.25D0) + a2CosXe*dcos(doy*4*PI/365.25D0)

! calculate the asymmetric slant delay in m (Chen and Herring 1997)
      D = 1.D0 / ( dsin(ele)*dtan(ele) + 0.0032D0 ) &
         * ( graN *dcos(azi) + graE * dsin(azi) ) ! mm
```

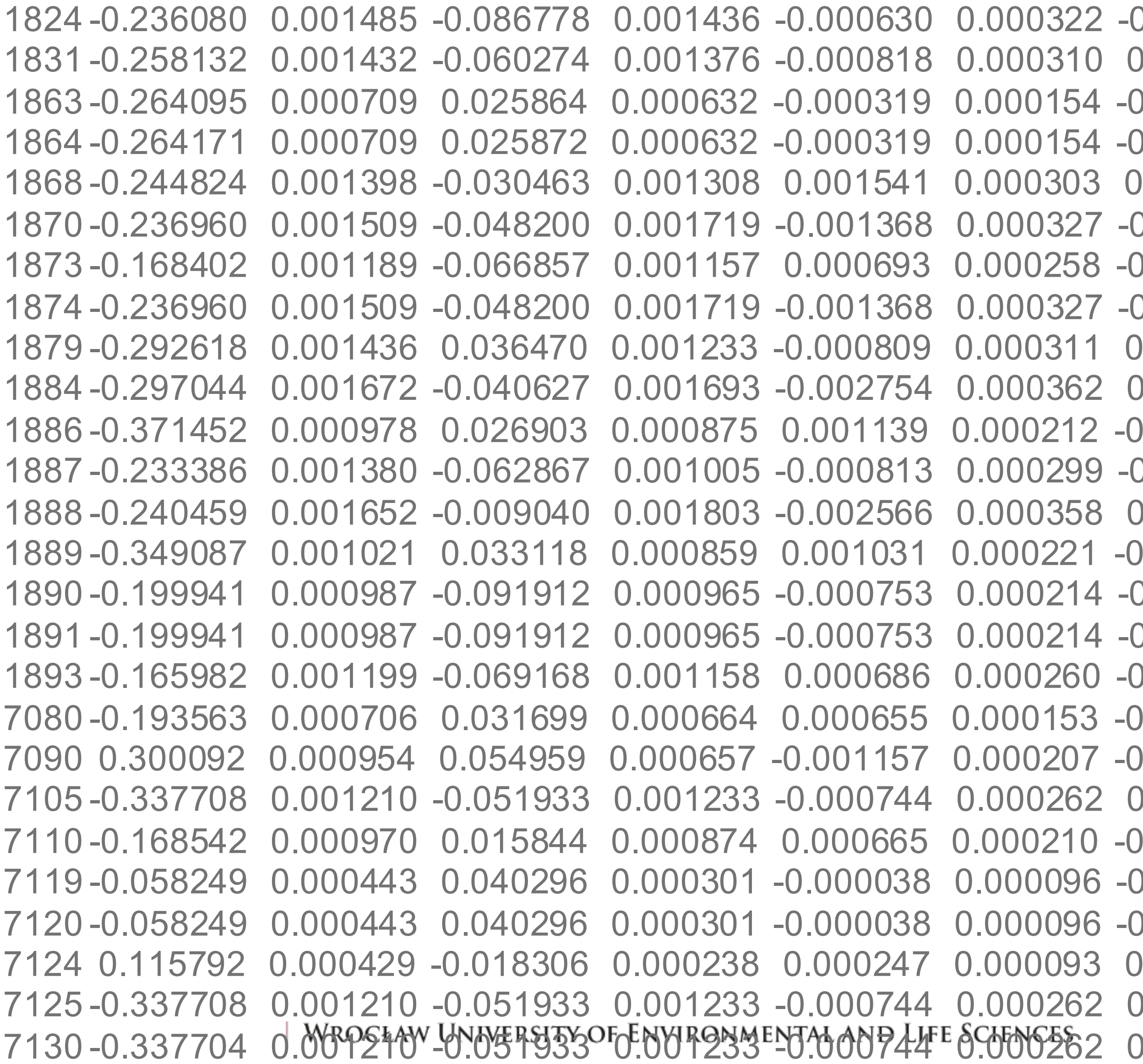

1824	-0.236080	0.001485	-0.086778	0.001436	-0.000630	0.000322	-0
1831	-0.258132	0.001432	-0.060274	0.001376	-0.000818	0.000310	0
1863	-0.264095	0.000709	0.025864	0.000632	-0.000319	0.000154	-0
1864	-0.264171	0.000709	0.025872	0.000632	-0.000319	0.000154	-0
1868	-0.244824	0.001398	-0.030463	0.001308	0.001541	0.000303	0
1870	-0.236960	0.001509	-0.048200	0.001719	-0.001368	0.000327	-0
1873	-0.168402	0.001189	-0.066857	0.001157	0.000693	0.000258	-0
1874	-0.236960	0.001509	-0.048200	0.001719	-0.001368	0.000327	-0
1879	-0.292618	0.001436	0.036470	0.001233	-0.000809	0.000311	0
1884	-0.297044	0.001672	-0.040627	0.001693	-0.002754	0.000362	0
1886	-0.371452	0.000978	0.026903	0.000875	0.001139	0.000212	-0
1887	-0.233386	0.001380	-0.062867	0.001005	-0.000813	0.000299	-0
1888	-0.240459	0.001652	-0.009040	0.001803	-0.002566	0.000358	0
1889	-0.349087	0.001021	0.033118	0.000859	0.001031	0.000221	-0
1890	-0.199941	0.000987	-0.091912	0.000965	-0.000753	0.000214	-0
1891	-0.199941	0.000987	-0.091912	0.000965	-0.000753	0.000214	-0
1893	-0.165982	0.001199	-0.069168	0.001158	0.000686	0.000260	-0
7080	-0.193563	0.000706	0.031699	0.000664	0.000655	0.000153	-0
7090	0.300092	0.000954	0.054959	0.000657	-0.001157	0.000207	-0
7105	-0.337708	0.001210	-0.051933	0.001233	-0.000744	0.000262	0
7110	-0.168542	0.000970	0.015844	0.000874	0.000665	0.000210	-0
7119	-0.058249	0.000443	0.040296	0.000301	-0.000038	0.000096	-0
7120	-0.058249	0.000443	0.040296	0.000301	-0.000038	0.000096	-0
7124	0.115792	0.000429	-0.018306	0.000238	0.000247	0.000093	0
7125	-0.337708	0.001210	-0.051933	0.001233	-0.000744	0.000262	0
7130	-0.337704	0.001210	-0.051933	0.001233	-0.000744	0.000262	0

VMF3o – details on provided data

Separated mapping functions:
(Boisits et al., 2020)

Hydrostatic:

$$m(e)_{VMF3oh} = \frac{1 + \frac{a_h}{1 + \frac{b_h}{1 + c_h}}}{sine + \frac{a_h}{sine + \frac{b_h}{sine + c_h}}},$$

Wet:

$$m(e)_{VMF3ow} = \frac{1 + \frac{a_w}{1 + \frac{b_w}{1 + c_w}}}{sine + \frac{a_w}{sine + \frac{b_w}{sine + c_w}}}$$

$$d_{atm\ h} = d_h \cdot m(e)_{VMF3oh}$$
$$+ m_{gh}(G_{Nh} \cdot cosA + G_{Eh} \cdot sinA)$$

$$d_{atm\ w} = d_w \cdot m(e)_{VMF3ow}$$
$$+ m_{gw}(G_{Nw} \cdot cosA + G_{Ew} \cdot sinA)$$

Hydrostatic delay:

Wet delay:

$$d_{atm} = (d_{atm\ h} + d_{atm\ w})$$

VMF3o – details on provided data

```
# Vienna Mapping Functions 3 optical (VMF3o) including discrete horizontal gradients calculated from
# ray-tracing data from the VieVS ray-tracer through OPERATIONAL NWM of the ECMWF.
#
# Reference:
# J. Boisits, D. Landskron and J. Boehm, VMF3o: the Vienna Mapping Functions for optical frequencies.
# J Geod (2020). https://doi.org/10.1007/s00190-020-01385-5
#
#
#
# columns:
# -------
# (1) station name
# (2) modified Julian date
# (3) hydrostatic mf coefficient a_h
# (4) wet mf coefficient a_w
# (5) zenith hydrostatic delay (m)
# (6) zenith wet delay (m)
# (7) pressure at the site (hPa)
# (8) temperature at the site (C)
# (9) water vapour pressure at the site (hPa)
# (10) hydrostatic north gradient Gn_h (mm)
# (11) hydrostatic east gradient Ge_h (mm)
# (12) wet north gradient Gn_w (mm)
# (13) wet east gradient Ge_w (mm)
#
1181     59580.00 0.00123089 0.00044140 2.4279 0.0019 1004.72  11.73  12.61  -0.567 -0.509   0.000  -0.001
1824     59580.00 0.00121898 0.00053376 2.3764 0.0020  983.40   4.70   7.66  -0.552 -0.359  -0.001   0.002
1831     59580.00 0.00121995 0.00063002 2.3516 0.0020  973.18   8.43   8.77  -0.511 -0.293   0.003  -0.001
1863     59580.00 0.00115922 0.00032986 1.7610 0.0006  727.54  -4.22   4.15  -0.233  0.174   0.002   0.001
1864     59580.00 0.00115916 0.00033379 1.7605 0.0006  727.34  -4.23   4.15  -0.233  0.173   0.002   0.001
1868     59580.00 0.00117473 0.00054096 2.3924 0.0002  990.39 -20.73   0.64  -0.167 -0.216  -0.001   0.001
1870     59580.00 0.00119806 0.00051963 2.3457 0.0010  970.89  -2.26   4.75  -0.575 -0.107  -0.002   0.001
1873     59580.00 0.00121770 0.00045928 2.3579 0.0014  975.13   5.22   7.77  -0.186 -0.388   0.001  -0.005
1874     59580.00 0.00119804 0.00052107 2.3455 0.0010  970.81  -2.26   4.75  -0.575 -0.107  -0.002   0.001
1879     59580.00 0.00118452 0.00061173 2.3860 0.0002  987.44  -8.68   0.93  -0.416  0.001   0.001  -0.000
1884     59580.00 0.00120372 0.00040681 2.4173 0.0013 1001.70   3.42   6.96  -0.616 -0.371   0.002   0.002
1885     59580.00 0.00120372 0.00040654 2.4174 0.0013 1001.72   3.42   6.96  -0.616 -0.371   0.002   0.002
1886     59580.00 0.00116850 0.00045088 1.9083 0.0006  789.02  -3.54   3.57  -0.285  0.109  -0.001  -0.001
1887     59580.00 0.00121324 0.00057953 2.4275 0.0005 1004.01  -7.84   3.04  -0.149 -0.036  -0.001   0.001
1888     59580.00 0.00119100 0.00042410 2.3875 0.0007  988.93  -2.32   4.55  -0.559 -0.257  -0.003  -0.000
1889     59580.00 0.00119677 0.00049358 2.1822 0.0010  902.51   2.86   4.52  -0.359  0.082  -0.002  -0.001
1890     59580.00 0.00117027 0.00061291 2.4554 0.0002 1015.62 -10.48   0.63  -0.594 -0.275   0.000  -0.000
1891     59580.00 0.00115367 0.00054793 2.3248 0.0002  962.46 -15.11   0.91  -0.536 -0.228   0.000   0.000
1893     59580.00 0.00122512 0.00049250 2.4445 0.0015 1010.95   7.73   8.15  -0.194 -0.383   0.001  -0.006
```

VMF Data Server
Vienna Mapping Functions Open Access Data

https://vmf.geo.tuwien.ac.at/trop_products/SLR/VMF3o/

https://vmf.geo.tuwien.ac.at/

Tropospheric parameters for each day and each SLR station generated on a operational basis with 6h-resolution based on numerical weather models

Latency of the operational products: 24h
(new data at about 18:00 every day for the previous day)

Predictions for the next day generated at 9:00, however, not publically available.

PMF – details on provided data

PMF includes a sophisticated model for the gradients (7 parameters):

$$d_{atm} = d^{z}_{atm} \cdot m_{PMF}(e) + (G_{Z0} + G_N \cdot \cos A + G_E \cdot \sin A$$
$$+G_{Z1} \cdot \cos 2A + G_{Z2} \cdot \sin 2A + G_{Z3} \cdot \cos 3A + G_{Z4} \cdot \sin 3A) \cdot m_g(e)$$

```
# Potsdam Mapping Functions Prime and gradients components of 1st and 2nd order.
# Balidakis, K., T. Nilsson, F. Zus, S. Glaser, R. Heinkelmann, Z. Deng, and H. Schuh (2018) Estimating integrated water vapor trends from VLBI, GPS, and numerical weather models: Sensitivity to tropospheric parameterization. Journal of Geophysical Research: Atmospheres, 123. https://doi.org/10.1029/2017JD028049
# Dousa, J., Dick, G., Kacmarik, M., Brokova, R., Zus, F., Brenot, H., Stoycheva, A., Muller, G., and Kaplon, J. (2016) Benchmark campaign and case study episode in central Europe for development and assessment of advanced GNSS tropospheric models and products, Atmos. Meas. Tech., 9, 2989-3008,
# Zus, F., M. Bender, Z. Deng, G. Dick, S. Heise,, M. Shangâ€Guan, and J. Wickert (2012) A methodology to compute GPS slant total delays in a numerical weather model. Radio Science, 47, RS2018. https://doi.org/10.1029/2011RS004853
# Zus, F., G. Dick, J. Dousa, and J. Wickert (2015) Systematic errors of mapping functions which are based on the VMF1 concept. GPS Solutions, 19( 2), 277-286.
# The ray-tracing was performed employing DNS, and ERA5 reanalysis fields (0.25Â°).
# DNS: Zus, F., G. Dick, J. Dousa, S. Heise, and J. Wickert (2014) The rapid and precise computation of GPS slant total delays and mapping factors utilizing a numerical weather model, Radio Sci., 49, 207-216
# a, b and c: total (hydrostatic + non-hydrostatic) mapping function coefficients
# ZHD: Zenith Hydrostatic Delay
# ZWD: Zenith Non-Hydrostatic Delay
# grdNS, grdEW: horizontal tropospheric gradient components of 1st order
# gradZ0, gradZ1, gradZ2, gradZ3, gradZ4: PMF prime parameters
# The current file was created by florian.zus@gfz-potsdam.de and kyriakos.balidakis@gfz-potsdam.de on 2019-09-25 10:41:12

# yyyy mm dd hh ______a[1] ______b[1] ______c[1] ___ZHD[m] ___ZWD[m] grdNS[mm] grdEW[mm] grdZ0[mm] grdZ1[mm] grdZ2[mm] grdZ3[mm] grdZ4[mm]
 1979 01 01 00 0.00119332 0.00279618 0.06205220 2.0707000 0.0007000 -0.735681 -0.286883  0.034893 -0.019186  0.007714 -0.020092  0.037296
 1979 01 01 06 0.00119190 0.00278582 0.06170286 2.0648000 0.0007000 -0.875033 -0.136525  0.080714 -0.026947  0.001167 -0.047941 -0.003693
 1979 01 01 12 0.00118890 0.00278216 0.06157932 2.0636000 0.0002000 -0.846771 -0.182847  0.060586 -0.035744  0.035648 -0.028063 -0.010469
 1979 01 01 18 0.00118824 0.00278977 0.06197476 2.0598000 0.0000000 -0.859615 -0.275793  0.036251  0.091769 -0.000016 -0.010367 -0.016120
 1979 01 02 00 0.00118142 0.00279453 0.06220177 2.0627000 0.0001000 -0.676747 -0.352601  0.047251  0.104782  0.029380  0.010039 -0.017986
 1979 01 02 06 0.00117441 0.00281239 0.06261456 2.0751000 0.0003000 -0.475482 -0.460147  0.139734 -0.001992  0.002399 -0.001097 -0.008662
 1979 01 02 12 0.00117013 0.00282070 0.06295670 2.0870000 0.0002000 -0.385181 -0.472819  0.092972 -0.008323 -0.002138  0.006802 -0.003569
 1979 01 02 18 0.00116893 0.00281737 0.06305501 2.0999000 0.0001000 -0.310430 -0.551629  0.020627 -0.024989  0.035406  0.024142 -0.001227
 1979 01 03 00 0.00117117 0.00280122 0.06263524 2.1049000 0.0001000 -0.608329 -0.520616 -0.155455  0.001684  0.117399  0.036726  0.016467
 1979 01 03 06 0.00117495 0.00278625 0.06221625 2.1022000 0.0001000 -0.466185 -0.591192 -0.098990  0.034435  0.074149  0.056429 -0.010608
 1979 01 03 12 0.00117999 0.00279967 0.06252595 2.1048000 0.0001000 -0.392462 -0.444006  0.043822  0.041679 -0.026695  0.008832 -0.011366
 1979 01 03 18 0.00118452 0.00278882 0.06216533 2.0985000 0.0001000 -0.422088 -0.206745 -0.005123  0.028059 -0.009329  0.005404 -0.013268
 1979 01 04 00 0.00118466 0.00278339 0.06191795 2.0904000 0.0008000 -0.390686 -0.046148 -0.010305  0.010437 -0.008014  0.010108  0.001052
```

Impact of troposphere delay modeling on ERPs determination

	X-pole		Y-pole		LOD	
	Offset	σ_mean	Offset	σ_mean	Offset	σ_mean
	µas		µas		µs/day	
With the estimation of the troposphere correction						
Mendes Pavlis	60	8.0	53	7.7	-43	5.5
Mendes Pavlis + par. grad.	42	8.0	31	7.7	-43	5.5
VMF3o ZWD	42	8.0	31	7.7	-43	5.5
PMF	41	8.0	30	7.7	-42	5.5
Without the estimation of the troposphere correction						
Mendes Pavlis	56	8.1	56	8.2	-42	5.5
Mendes Pavlis + par. grad.	35	8.1	32	8.2	-40	5.5
VMF3o ZWD	38	8.1	32	8.1	-41	5.4
PMF	38	9.4	31	8.1	-41	5.5

Geocenter differences w.r.t. M-P model without ZTD estimation

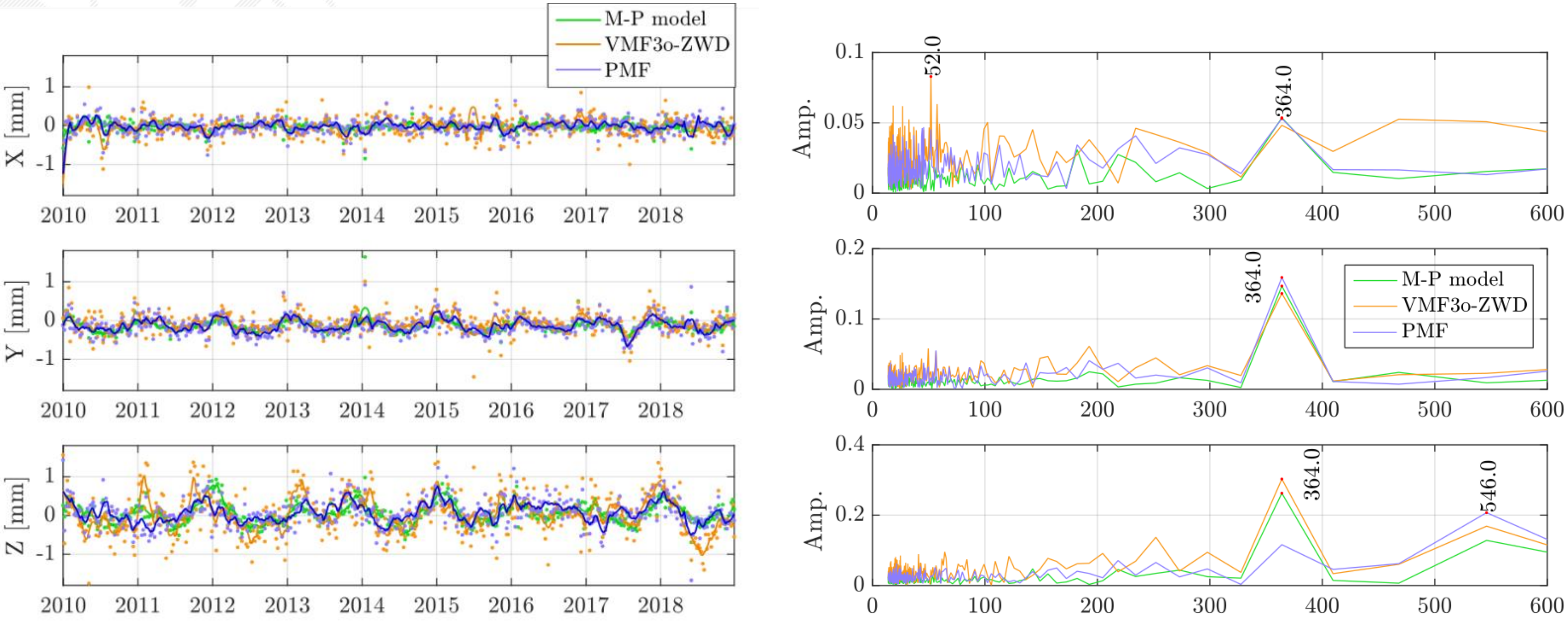

	X [mm]		Y [mm]		Z[mm]	
	offset	amplitude	offset	amplitude	offset	amplitude
Mendes – Pavlis	0.7	2.9	1.4	2.0	-1.7	3.7
Mendes – Pavlis + grad. m	0.6	2.9	1.3	2.0	-1.7	4.0
VMF3o ZWD	0.6	3.0	1.4	2.1	-1.7	4.0
PMF	0.6	2.9	1.3	2.0	-1.7	3.7
Mendes – Pavlis (with TRP est.)	0.6	3.0	1.0	2.1	-2.4	3.4

Comparison of mapping functions and hor. gradients VMF3o, PMF, MP

Gradients

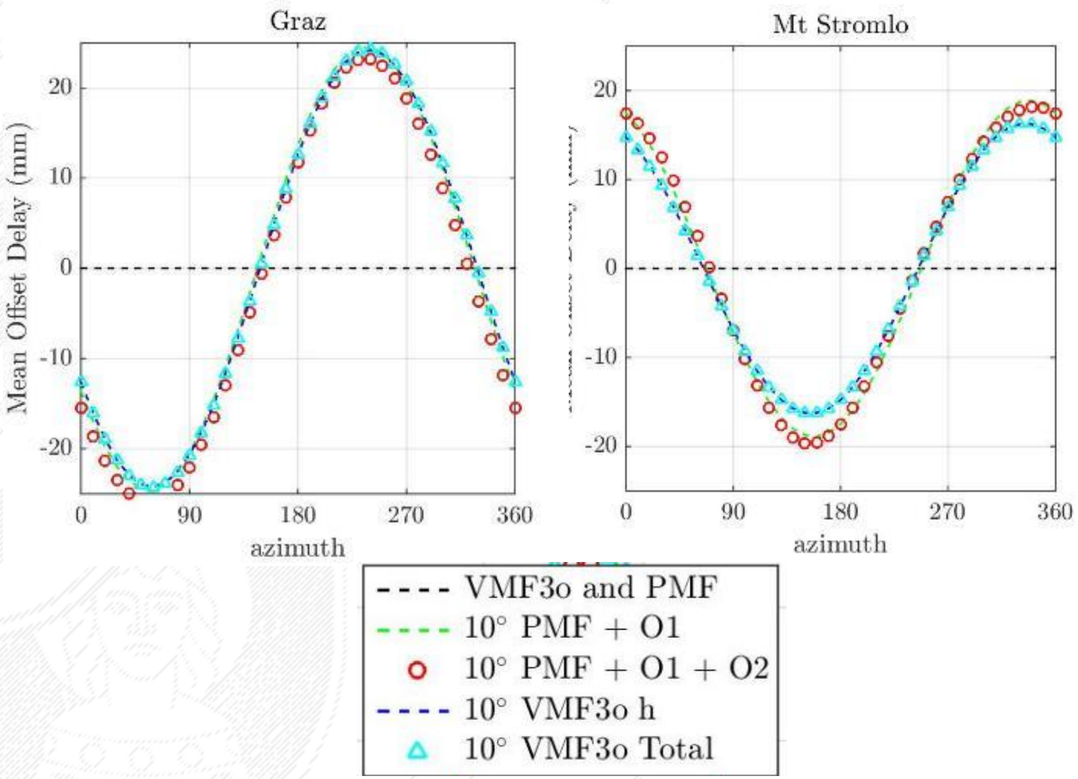

Mapping Functions

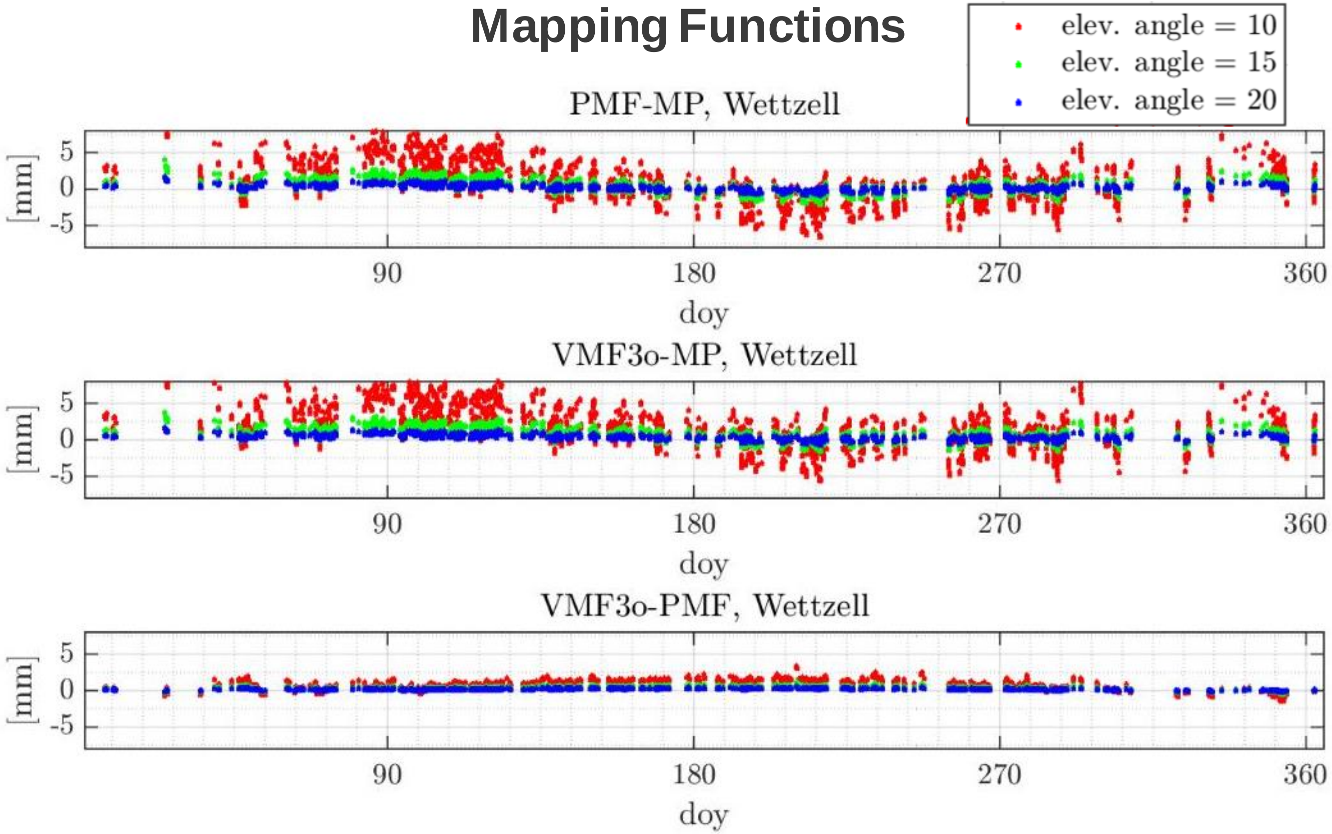

Differences between PMF, VMF3o and FCULa (MP) mapping functions.

Despite differences in models, PMF and VMF3o provide similar slant delays.

However, there are substantial differences between MP (based on in-situ data) and PMF&VMP3o (both based on NMW).

SLR validation of SWARM GPS-based orbits

Kinematic AIUB orbit   Reduced-dynamic AIUB orbit

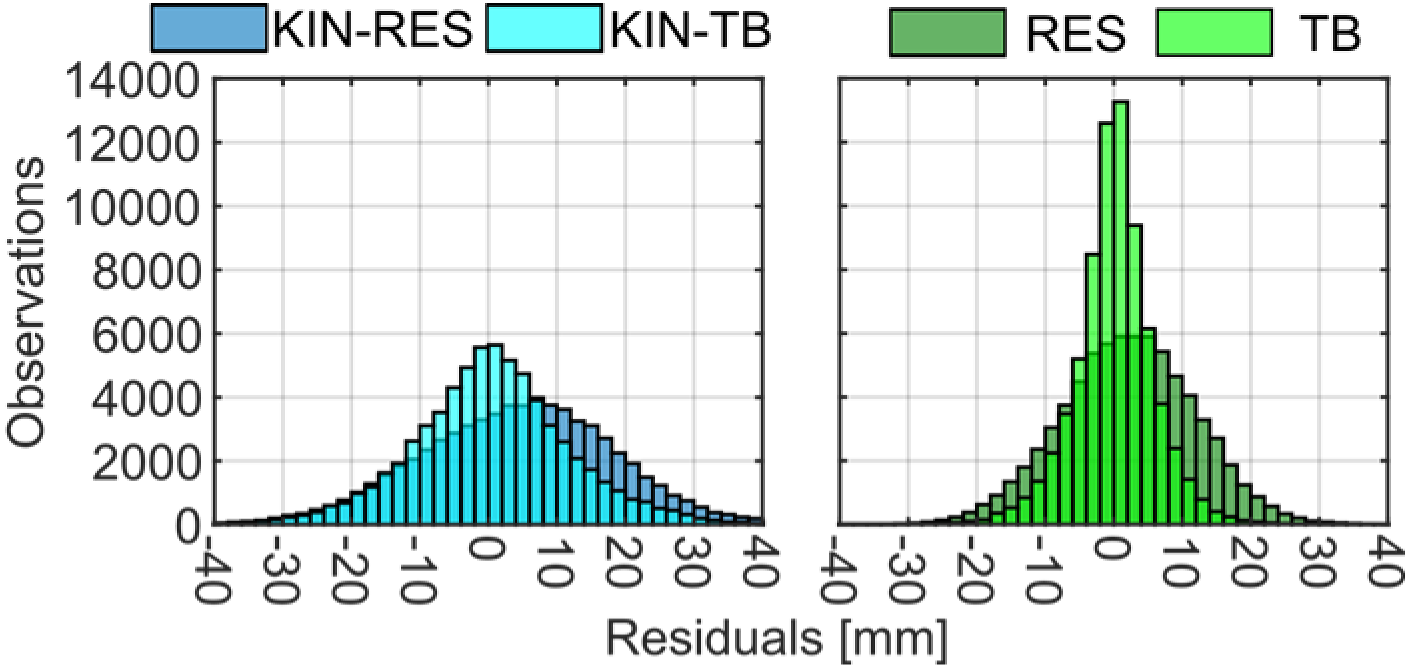

From **49%** to **66%**
of residuals within
+/-10mm

From **68%** to **91%**
of residuals within
+/-10mm

Introducing **troposphere biases allows for the comparison of the orbit quality** between kinematic and reduced-dynamic orbits. SLR observations are freed then from elevation-dependent errors.

The differences of the quality of GPS-based orbits become more obvious.

After the correction of tropospheric biases, the STD of SLR residuals is equal to 5 mm for 12 high-performing SLR stations and reduced dynamic orbits (15 mm in the standard solution).

RES – standard solution
TB – with the estimation of tropospheric biases

Strugarek et al. (2022) ***Satellite Laser Ranging to GNSS-based Swarm orbits with handling of systematic errors***, GPS Solutions, 26(104)
https://doi.org/10.1007/s10291-022-01289-1

Time series of: TRP, RGB and Up component – Wettzell (without an artificial bias)

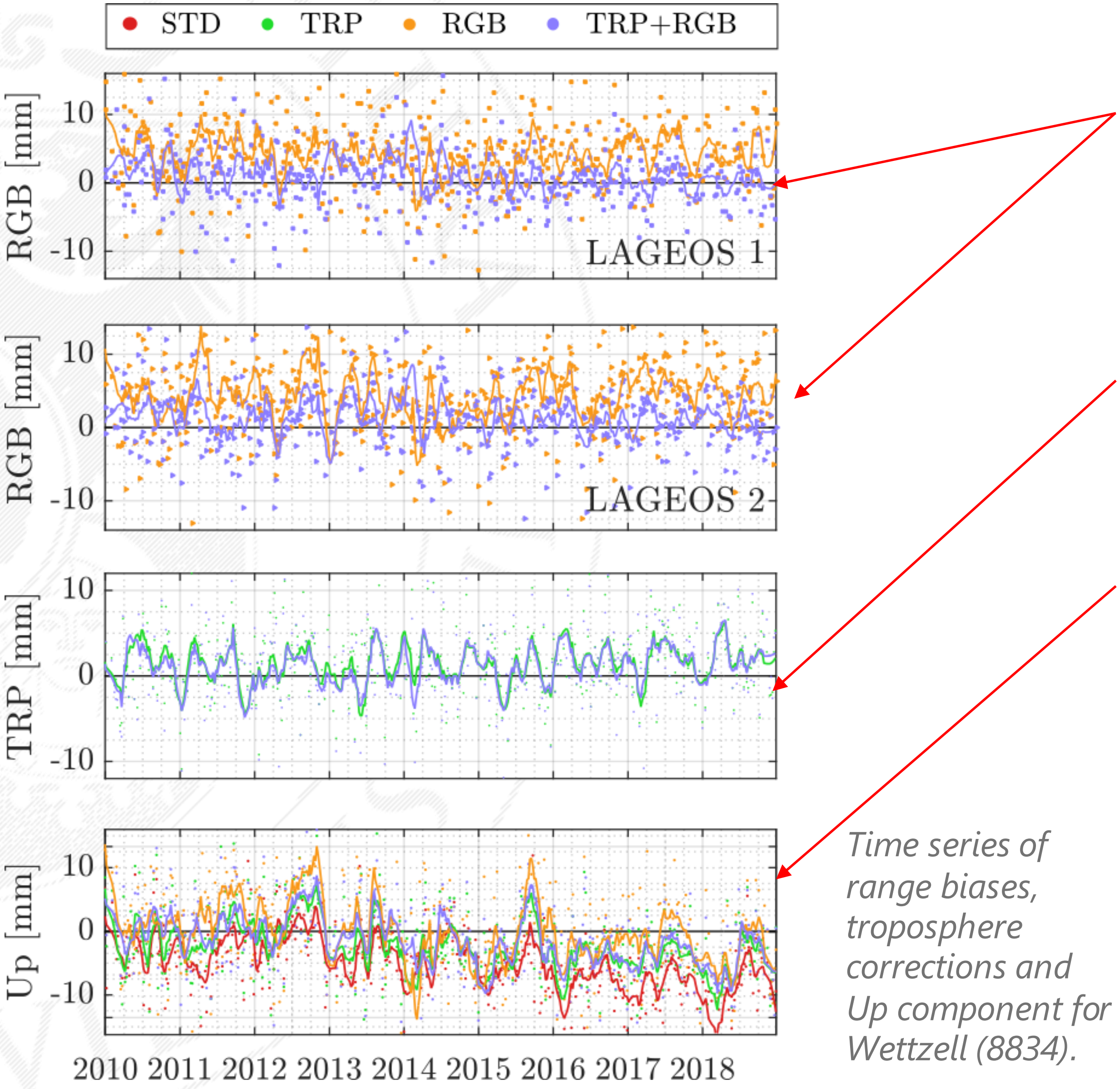

Time series of range biases, troposphere corrections and Up component for Wettzell (8834).

- Estimation of troposphere correction significantly reduces standard deviation of range biases,
- Estimation of range biases does not deteriorate the troposphere correction,
- Estimation of troposphere delay corrections improves IQR station coordinate repeatability, whereas RGB overestimates the Up component correction.